International Journal of Engineering &Technology, 7 (4) (2018) 6481-6487

International Journal of Engineering & Technology

Website: www.sciencepubco.com/index.php/IJET
doi: 10.14419/ijet.v7i4.24457
Research paper

Optimization and prediction of laser micro-grooving by artificial neural network

Sivaraos [1] *, A. Z. Khalim [1], Yusliza Yusoff [2], S. Pujari [3], D. Sivakumar [4], M. A. Amran [1]

[1] *Advanced Manufacturing Centre, Faculty of Manufacturing Engineering, University Technical Malaysia Melaka*
[2] *School of Computing, Faculty of Engineering,81310 UTM Skoda, Johor Bahru, Johor*
[3] *Faculty of Mechanical Engineering, Lendi Institute of Engineering and Technology, Vizianagaram, Vizag, India*
[4] *Centre for Advanced Research on Energy, Faculty of Mechanical Engineering, University Technical Malaysia Melaka*
**Corresponding author E-mail: sivarao@utem.edu.my*

Abstract

Lasers are widely used in machining industry as a cutting tool ultra-flexible, produce high quality end product, quick set up, non-mechanical contact between the workpiece and the tool, and small size of the heat affected zone are some of the good features of laser cutting. However, laser cutting of sheet metal has limitation in machining of circular geometries by turning operation. There-fore, a novel approach has been devised to investigate in transforming a 2D flatbed CO2 laser cutting machine into 3D laser lathing capability as an alternative solution. In this paper, artificial neural networks (ANN) were employed to build a predictive model for depth quality of micro-grooving commercially pure (CP) titanium grade 2 by using a flatbed (CO2) laser cutting. The predicting model includes five input variables of the power, the gas pressure, the cutting speed, the focal distance and the depth of cut. It is found that from the ANN model developed, near optimum groove depth values are generated where the average prediction error is 6.48%.

Keywords: *CO2 Laser Cutting; Laser Lathing; Micro-Grooving; Neural Network; Optimization.*

1. Introduction

Laser cutting is one of the advanced machines which are capable of processing almost any kind of materials with high degree of flexibility and precision. It is commonly used in precision industries as it has the ability to cut complex profiles featuring extra ordinary shapes, corners, slots, and holes with high degree of repeatability and small region of heat affected zone (HAZ) [1]. In term of machining, laser also known as a process involving laser beam as the heat source and a thermal process used to remove materials without mechanical engagement with the workpiece, instead, it is heated up to the melting point and remove the melt by high pressure gas ejection, vaporization, or ablation mechanisms [2]. With great advantages of laser machining, the drawback of conventional lathe especially in performing a narrow cavity of a certain depth on a cylindrical part can be overcome.

Thus, in order to have a better control of the micro groove on a cylindrical part, laser is found to be most suitable as it processes the materials without having any mechanical contact between the laser beam (virtual tool) and the spinning work. So to understand the behavior and scientific reasoning behind the actual processing phenomenon, an intelligent system called Artificial Neural Network (ANN) is a powerful tool in modelling the environment to predict the response. Since the three axes laser machine is too expensive, thus, a two axes (2D) flat-bed 3KW CO2 laser machine has been modified into three axes (3D) as an alternative to perform laser grooving.

The removal of a single layer is achieved using multiple overlapping straight grooves where the groove profile has been predicted by theoretical models before the work was carried out [3]. Layer by layer peeling concept for three dimensional laser machining of micro parts using laser turning machine has been carried out by controlling three main parameters namely power, repetition rate and speed of laser process [4]. Besides that, the process parameters relationship of pulsed Nd:YAG laser-turning operation for production of micro-groove on cylindrical workpiece was investigated by considering air pressure, lamp current, pulse frequency, pulsed width and cutting speed as correspondence controllable parameters [5].

A strategy for predicting the optimum machining parameter setting for the generation of the maximum depth of groove with minimum height of recast layer has been present. A cascade forward back-propagation neural network is used to construct the laser beam machining (LBM) process model and found that the use of ANN architecture 4-25-2, one hidden layer can provide a best prediction [6]. An optimization of surface roughness has been studied and model using ANN approach. The model shows that architecture 4-7-1 gives an optimum quality cut of surface roughness by controlling four cutting variables namely laser power, cutting speed, assist gas pressure, and work piece thickness. It also found that the importance of cutting speed is more dominant in optimizing the surface roughness as compared with other cutting variable [7]. The optimal turning parameters of AA2024-T351 alloy namely cutting speed, feed rate, tool rake angle, and contact friction coefficient is investigated through Abaqus/Explicit numerical simulations and optimized with ANN models. Result shows that the performance of the ANN models demonstrated the fidelity of solving and predicting the optimum process parameters [8].

An artificial neural network (ANN) model has been developed to predict the process criteria and using multi-objective optimization, the process parameter was carried out to achieve the desired surface roughness and minimum micro-turning depth deviation. It was found that the developed ANN model can predict the process criteria more accurately than response surface methodology

(RSM) [9]. The predicting model for six laser-cutting qualities of QFN package has been done using back-propagation neural network. Four algorithms including Broyden Fletcher Goldfarb Shanno Quasi-Newton (BFG), Scaled Conjugate Gradient (SCG), Gradient Descent (GD) and Levenberg-Marquardt LM algorithms are used to simulate the model. Results shows that, LM algorithm is an optimal algorithm which is less predicting error compared to other improving algorithms [10]. Taguchi method is used to optimize an artificial neural network model trained by Levenberg-Marquardt algorithm. Analysis and experiments shows that the optimal ANN training and architectural parameters can be determined in a systematic way, ultimately avoiding the lengthy trial and error procedure [11].

A hybrid GA-Taguchi-ANN optimization model has been developed. It is constructed in such a way to realize mutual input output through ANN and GA. Results shows that the developed GA-Taguchi ANN model could reduce the maximum prediction error below 10% [12]. The effect of process parameters of Nimonic C-263 super alloy during machining using die sinking EDM has been studied. All the machining and process parameters are modelled by ANN and found that an architecture 6-6 is adopt as an optimal parameter [13]. ANN was used to predict methane yield with different operating parameters. The model is based on the feed forward network (FFN) with one hidden layers. It shows that ANN models are better tool for optimizing the methane content from different factors [14]. The prediction model of refined palm oil quality has been investigated for online quality monitoring purposes. Each network shows that different number of hidden nodes gave different prediction performance of both R and MSE [15]. Based on the literature survey, there are many methods used in optimization of ANN model. It is observed that ANN model is found to be suitable in modeling non-linearity problem because it has powerful pattern classification and pattern recognition capabilities [22]. In this paper a clearly step by step optimization of laser cutting model based on ANN are introduced in order to optimize the non-linear cutting profile.

2. Theoretical model of laser cutting

In laser cutting, laser beam penetrates through the entire thickness of the workpiece and advances parallel to the surface of the workpiece [16]. A cutting model was developed based on the absorptivity calculated over the cutting kerf [17]. Meanwhile, a relationship between the power density incident on a material and the resulting cutting speed was developed and found that, to maximize cutting speed and energy utilization, the jet diameter should be smallest possible consistent with an attainable power density [18]. Based on the balance between absorbed power of beam, power for melting material, power for heating material, and conduction heat losses, a laser erosion front model was formulated and there are some assumptions for this model [16]:

- The kerf width is assumed to be constant with the laser beam diameter
- The contour lines of the erosion front can be described by semi-circles with radius equal to the beam radius
- The inclination angle of the erosion front is constant and determined experimentally
- The erosion front is assumed to have a linear slope

The first step in this study is to determine the absorptivity of the erosion front where the refractive index and absorption coefficient can be defined [19]. The theoretical models of laser cutting are given as below equations (1) – (9)

Refractive index, n:

$$n = \left(0.5\left(\left(\left(1-\frac{\omega_p^2}{v^2+\omega^2}\right)^2+\left(\frac{v\omega_p^2}{\omega(v^2+\omega^2)}\right)^2\right)^{1/2}+\left(\frac{1-\omega_p^2}{v^2+\omega^2}\right)\right)\right)^{1/2} \quad (1)$$

Absorption coefficient, α:

$$\alpha = \left(0.5\left(\left(\left(1-\frac{\omega_p^2}{v^2+\omega^2}\right)^2+\left(\frac{v\omega_p^2}{\omega(v^2+\omega^2)}\right)^2\right)^{1/2}\left(\frac{1-\omega_p^2}{v^2+\omega^2}\right)\right)\right)^{1/2} \quad (2)$$

where ω is the laser frequency, ω_p is the plasma frequency, and v is the electron collision frequency. A complex refractive index can be defined equation (3).

Refractive index, n*:

$$n^* = n + i\alpha \frac{c_0}{2\omega} \quad (3)$$

where, C_o is the speed of light and i = (-1)1/2. The absorptivity of the melt film at the erosion front can be expressed as equation (4).

Absorptivity, A_s:

$$A_s = 1-\left(\frac{\cos\delta-(n^{*2}-\sin^2\delta)^{1/2}}{\cos\delta+(n^{*2}-\sin^2\delta)^{1/2}}\right)^2 \quad (4)$$

Where, δ is the angle of incidence of the laser beam on the erosion front. If the mode, polarization and focal shape of the beam are known, then the variation of absorptivity on the erosion front can be determined as:

$$A(z,\beta)p_{Laser} = \cos\delta\, A(n^*,\delta)\, I(z,\beta) \quad (5)$$

With, A (z, β)P_{Laser} is the absorbed beam intensity, β is the circular angle, z is the depth from the top surface, and I(z, β) is the incident beam intensity. An overall absorptivity for the erosion front can be found by integrating the absorbed laser power over the erosion front area and dividing by the total laser power. The erosion front shape can be determined through a power balance between laser power and the rates of heating, melting, and thermal loss. Material removal is assumed to occur through completely melting; no material is vaporized.

$$A(z,\beta)p_{Laser} = p_r + p_m + p_1 \quad (6)$$

Thus, P_{Laser} is the total laser power and the heating power is:

$$p_T = b_s sV\rho c(T_p - T_0) \quad (7)$$

the melting power is

$$p_m = b_s sV\rho\varepsilon_m \quad (8)$$

and the heat conduction loss is

$$p_1 = \frac{\pi k(T_m-T_0)\sqrt{b_s s}}{\arctan\left(\frac{16\kappa}{Vs}\right)^{1/2}}\exp\left(-\frac{Vb_s}{2\kappa}\right) \quad (9)$$

Using Eq. (9) of power balance, the cutting depth can be solved to determine the shape of erosion front where s is the cutting depth, b_s is the kerf width, T_m is the melting temperature, T_0 is the ambient temperature, and V is the scanning velocity. Material properties include the thermal conductivity k, thermal diffusivity κ, density ρ, specific heat c, melting temperature T_m, and heat of fusion $\boldsymbol{\varepsilon_m}$.

3. Experimental details

The transformation 2D to 3D laser lathe has been done successfully and the performance also was validated by precisely setup between a tangential insertion of laser beam and spinning workpiece on the sacrificial table. The details of CO2 laser machine specification are shown in Table 1, while the experimental setup is shown in Figure 1. Throughout these experimentations, constant and variable processing parameters were identified.

Table 1: CO2 Laser Machine Specification

Machine	Specification
Manufacturer	LVD Company N.V, Belgium
Model	Helius-2513
Brand	LVD Helius
Envelope	2500x1250 mm
Maximum speed	250 mm/s
Maximum laser power	3 kW

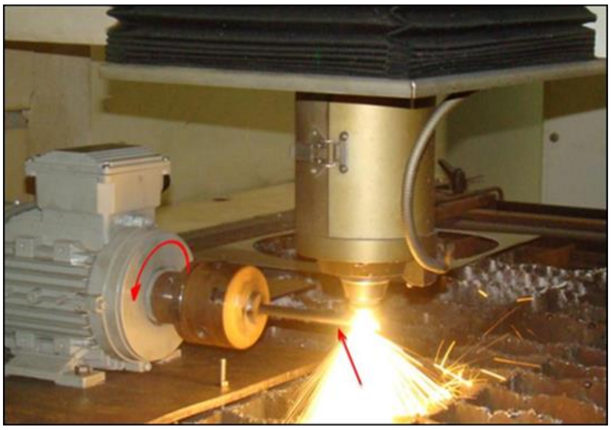

Fig. 1: Laser Micro-Groove of Grade 2 Titanium.

Table 2 shows the laser process parameters, while Table 3 presents the design parameters namely power (P), gas pressure (G), cutting speed (V), depth of cut (d) and Focal distance (F) which were varied through-out the experiments. Table 4 shows the material properties of CP Ti G2. A summary of 96 experimental designs is given in Table 5 and it was done using response surface methodology (RSM).

Table 2: Laser Process Parameters Constant

Laser Processing	Value
Frequency	1850 Hz
Duty cycle	80 %
Laser mode	Continuous wave
Stand-off distance	1 mm
Nozzle type	Cylindrical
Beam diameter	0.5 mm
Gas jet selection	Nitrogen
Focus lens	7.5 mm
Nozzle diameter	1.2 mm

parameters are capable to capture using artificial neural network (ANN).

ANN can be categorized as a black box model which provides information behind physics process explicitly [20]. ANN model has the computational ability of non-linear problems and has been widely used to predict and optimize the laser micro-grooving process using modified CO2 laser cutting machine. But none of the authors have explored in transforming flatbed CO2 laser cutting machine into 3D laser lathing which works on micro-grooving of commercially pure (CP) titanium grade 2. Some of researchers has been done laser micro-grooving but they used difference kind of machine, materials and method. In this model, a network consists of three layers; an input layer, a hidden layer and an output layer as illustrated in Figure 3. There are five (5) neuron which are corresponds to five input process parameters that have been already enlisted in Table 3. The output layer consists of one neurons, which correspond to the output responses namely groove depth (GD). The selection of the number of neuron in the hidden layer is the crucial part. Careful selection of hidden layer neuron is important in order to achieve better best fit model performance. The best fit model ensures the near desired solutions are created with least number of iterations and minimum prediction error. The results obtained from ANN model are analysed and compared with the real experimental results by calculating the prediction error. The prediction error can be defined as follows:

Prediction error (%):

Table 3: Design Parameters

Factors	Unit	Low	Medium	High
Power (P)	watt	1500	1650	1800
Gas Pressure (G)	bar	17	18	19
Cutting Speed (V)	mm/min	700	800	900
Depth of Cut (d)	mm	0.25	0.48	0.7
Focal Distance (F)	-	-2	-1	0

Table 4: Material properties of Commercially Pure (CP) Titanium Grade 2

C %	Fe %	H %	N %	O %	Ti%
0.1 Max	0.3 Max	0.015 Max	0.03 Max	0.25 Max	99.2

The performance of laser machining plays an important role in producing reliable quality measures. So in order to cater the desired depth of micro-grooving, an optical comparator was used to measure the groove depth as shown in Figure 2.

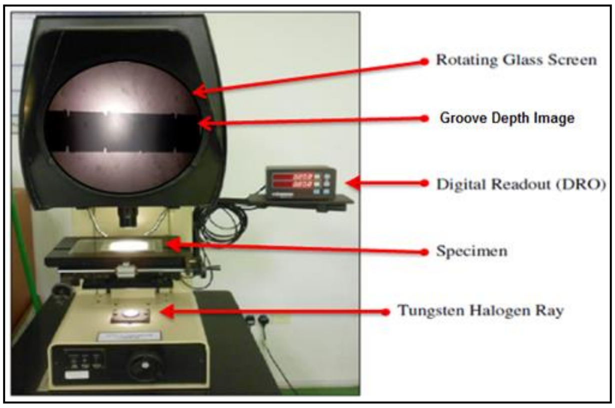

Fig. 2: Groove Depth Measurement with Optical Comparator.

4. ANN modelling

One of the purposes of modelling development is to minimize the cost of production especially in precision industries which is commonly involved in the machining process. Based on preliminary investigation, the input and output parameter has been tested via experimentation before comes into real machining. With the high-end technologies, the relationships between input and output

(Experimental result-Predicted results)/(Experimental results) (10)

A neural network toolbox was used for training and testing of the simulations data. Since the total number of experiment data is 96 (Table 5), 83 data were considered for ANN training and the rest were used for ANN testing. The standard network type which is feed forward back-propagation was used in development of ANN.
For the proposed ANN architecture, the numbers of neurons in the hidden layers were determined through a trial-and-error method. The ANN predicted outcomes were evaluated by considering the minimum percentage of prediction error. In order to get tangible outcomes without trail-and-error method, a flow of parameters and architecture selection of ANN model has been designed (Figure 4).

5. Result & discussion

5.1. ANN optimization

Figure 4 shows the step-in selection of neural network parameter. There are six (6) steps which are involved in getting an optimal neural network parameter for this investigation.
Step one (1): is classify network type, feed-forwards back-propagation has been selected as network type since the weights and biases were adapted to minimise the mapping error and it also can be applied to almost all applications in the manufacturing domain [21,22].

Step two (2): After determining the network type, next step is identifying an algorithm. In this section four (4) algorithms which are
Levenberg-Marquardt (LM), BFGS Quasi-Newton (BFG), Scaled Conjugate Gradient (SCG), and Gradient Descent (GD) used to simulate, then choose optimal algorithm that has less predicting error to train ANN and obtain an ANN predicting model. The algorithm is selected randomly, and some has frequently used by researcher [23]. Based on observation, it shows that LM algorithm gives lower percentage of average predicting error compare to others algorithm. LM algorithm is fast and good in searching near optimum solutions for a variety of problems compared other algorithms. Besides, LM also obtains better performance, convergence and accurate predicting values [10]. Figure 5 shows the comparison average predicting errors of ANN models between four algorithms.

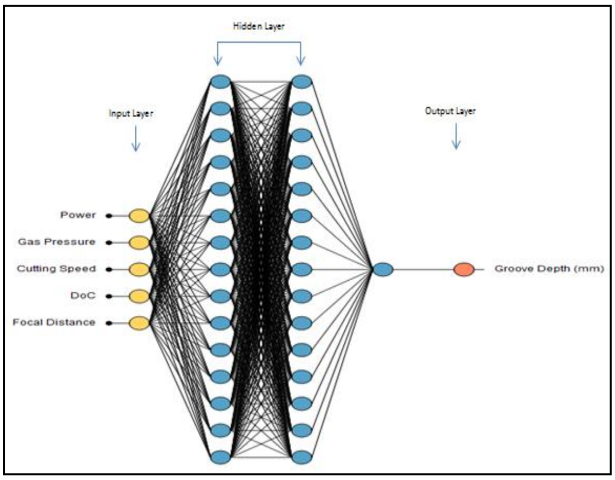

Fig. 3: ANN Architecture of 5-15-1with 5 Inputs, 2 Hidden Layer and Singleton Output.

Table 5: Experimental Design and Observed Response by RSM

No	P	G	V	d	F	GD	No	P	G	V	d	F	GD	No	P	G	V	d	F	GD
1	1800	190	700	0.25	0	0.16	33	1650	180	800	0.48	-1	0.41	65	1650	180	700	0.48	-1	0.49
2	1650	180	800	0.48	-1	0.39	34	1650	180	800	0.25	-1	0.21	66	1800	190	900	0.25	-2	0.24
3	1800	190	700	0.70	-2	0.66	35	1500	190	700	0.25	-2	0.15	67	1500	170	900	0.70	0	0.64
4	1650	180	800	0.48	-2	0.41	36	1650	180	800	0.48	-1	0.4	68	1650	180	900	0.48	-1	0.48
5	1500	190	900	0.25	0	0.12	37	1800	170	900	0.25	0	0.22	69	1650	180	700	0.48	-1	0.51
6	1650	180	800	0.48	-1	0.43	38	1650	180	800	0.70	-1	0.72	70	1800	170	700	0.25	-2	0.3
7	1500	180	800	0.48	-1	0.44	39	1650	180	800	0.48	0	0.37	71	1800	190	900	0.70	0	0.69
8	1650	180	800	0.48	-2	0.44	40	1800	170	700	0.70	0	0.61	72	1650	180	800	0.48	-1	0.41
9	1650	190	800	0.48	-1	0.45	41	1800	170	900	0.25	0	0.22	73	1500	170	900	0.25	-2	0.16
10	1500	190	700	0.70	0	0.69	42	1650	170	800	0.48	-1	0.38	74	1800	190	900	0.25	-2	0.23
11	1800	190	900	0.25	-2	0.23	43	1650	180	800	0.48	-2	0.43	75	1800	170	700	0.25	-2	0.25
12	1800	170	700	0.70	0	0.73	44	1500	170	900	0.70	0	0.58	76	1500	190	900	0.70	-2	0.64
13	1650	180	800	0.48	-1	0.48	45	1650	180	800	0.48	-1	0.43	77	1650	180	800	0.25	-1	0.21
14	1500	170	900	0.25	-2	0.2	46	1500	180	800	0.48	-1	0.4	78	1500	170	700	0.70	-2	0.66
15	1500	170	700	0.70	-2	0.68	47	1800	180	800	0.48	-1	0.48	79	1500	190	900	0.70	-2	0.67
16	1500	170	700	0.25	0	0.24	48	1650	170	800	0.48	-1	0.47	80	1500	170	900	0.25	-2	0.2
17	1650	180	800	0.48	-1	0.49	49	1800	170	900	0.70	-2	0.65	81	1650	180	800	0.48	-1	0.48
18	1800	170	900	0.70	-2	0.66	50	1650	180	800	0.48	-1	0.45	82	1650	180	800	0.48	-1	0.49
19	1650	180	800	0.48	-1	0.46	51	1650	180	900	0.48	-1	0.42	83	1650	170	800	0.48	-1	0.49
20	1500	170	700	0.25	0	0.13	52	1800	170	700	0.70	0	0.72	84	1650	180	800	0.25	-1	0.23
21	1650	180	800	0.48	-1	0.39	53	1800	190	700	0.25	0	0.25	85	1500	190	900	0.25	0	0.17
22	1500	180	800	0.48	-1	0.35	54	1650	180	800	0.48	-1	0.49	86	1500	190	700	0.70	0	0.7
23	1650	180	800	0.48	-1	0.44	55	1500	190	900	0.70	-2	0.64	87	1500	170	900	0.70	0	0.66
24	1800	190	700	0.25	0	0.2	56	1800	170	700	0.25	-2	0.26	88	1650	180	800	0.48	-1	0.52
25	1500	190	900	0.25	0	0.13	57	1800	190	900	0.70	0	0.72	89	1650	180	800	0.48	0	0.5
26	1800	180	800	0.48	-1	0.51	58	1500	190	700	0.70	0	0.59	90	1650	180	800	0.70	-1	0.71
27	1650	180	700	0.48	-1	0.52	59	1800	190	900	0.70	0	0.61	91	1650	190	800	0.48	-1	0.48
28	1500	170	700	0.25	0	0.18	60	1800	190	700	0.70	-2	0.63	92	1650	190	800	0.48	-1	0.44
29	16	18	80	0.	-1	0.	61	18	17	90	0.	0	0.	93	16	18	80	0.	-1	0.

	50	0	0	48		46		00	0	0	25		22		50	0	0	70		65
30	1800	190	700	0.70	-2	0.71	62	1500	190	700	0.25	-2	0.2	94	1800	180	800	0.48	-1	0.47
31	1800	170	900	0.70	-2	0.73	63	1500	190	700	0.25	-2	0.23	95	1650	180	800	0.48	-1	0.49
32	1650	180	800	0.48	0	0.44	64	1650	180	900	0.48	-1	0.48	96	1500	170	700	0.70	-2	0.6

* P; Power, V; Cutting Speed, G; Gas Pressure, F; Focal Distance, D; Depth of Cut and GD; Groove Depth

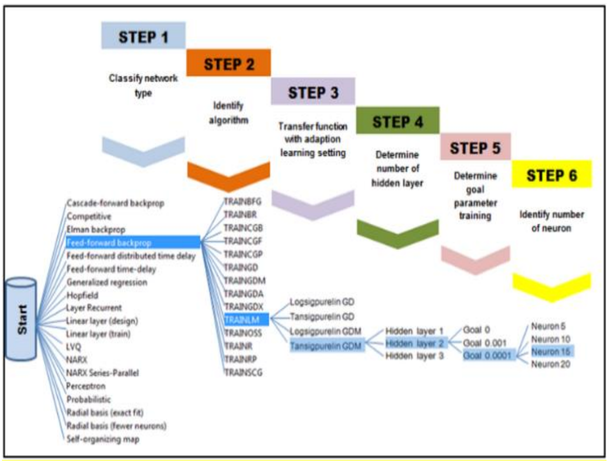

Fig. 4: ANN Model Development Parametrical Architecture.

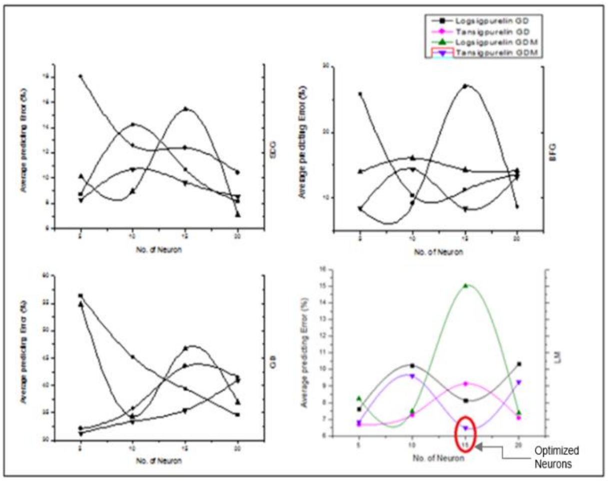

Fig. 5: Comparison Average Predicting Error between Algorithms LM, BFG, SCG and GD.

Step three (3): The next step to optimize the neural network parameter is decided the transfer function and learning adaption. There are three (3) types of transfer function which is Log-Sigmoid (logsig), Tan-sigmoid (tansig) and Linear (purelin) while there are two type of adaption learning function which is gradient descent learning (learnGD) and gradient descent with momentum learning (learnGDM). However, [12] mention that learnGD is not very effective compare to learnGDM. For input layer, logsig and tansig transfer function was used while purelin transfer function used for output layer. The combination between transfer function and learning adaption create four type of transfer function with learning adaption which are logsig-purelin with GD, tansig-purelin with GD, logsig-purelin with GDM and tansig-purelin with GDM.
By referring graph in Figure 5, it shows that tansig-purelin with GDM has low percentage of average predicting error for all four (4) algorithm, means that tansig-purelin with GDM gives significant impact to the development of ANN model. This fact also supports by [24] where gradient descent with momentum provides better data fitting capability

Table 6: Comparison between Experimental and ANN Predicted Results of Training Data for Groove Depth

No	Exp.	ANN Predicted	Percentage Error (%)	No	Exp.	ANN Predicted	Percentage Error (%)	No	Exp.	ANN Predicted	Percentage Error (%)
1	0.16	0.22	37.50	29	0.22	0.22	0.00	57	0.64	0.63	1.56
2	0.39	0.46	17.95	30	0.72	0.71	1.39	58	0.48	0.45	6.25
3	0.66	0.64	3.03	31	0.37	0.43	16.22	59	0.51	0.51	0.00
4	0.41	0.43	4.88	32	0.61	0.61	0.00	60	0.3	0.25	16.67
5	0.43	0.46	6.98	33	0.22	0.22	0.00	61	0.69	0.67	2.90
6	0.44	0.35	20.45	34	0.38	0.47	23.68	62	0.16	0.18	12.5
7	0.45	0.46	2.22	35	0.43	0.43	0.00	63	0.23	0.23	0.00
8	0.69	0.64	7.25	36	0.58	0.63	8.62	64	0.25	0.25	0.00
9	0.23	0.23	0.00	37	0.43	0.46	6.98	65	0.64	0.66	3.13
10	0.48	0.46	4.17	38	0.4	0.35	12.5	66	0.21	0.21	0.00
11	0.2	0.18	10.0	39	0.48	0.49	2.08	67	0.66	0.63	4.55
12	0.68	0.63	7.35	40	0.47	0.47	0.00	68	0.67	0.66	1.49
13	0.49	0.46	6.12	41	0.65	0.66	1.54	69	0.2	0.18	10.0
14	0.66	0.66	0.00	42	0.45	0.46	2.22	70	0.48	0.46	4.17
15	0.13	0.15	15.38	43	0.42	0.45	7.14	71	0.49	0.46	6.12
16	0.39	0.46	17.95	44	0.25	0.22	12.00	72	0.49	0.47	4.08
17	0.35	0.35	0.00	45	0.49	0.46	6.12	73	0.23	0.21	8.70
18	0.44	0.46	4.55	46	0.64	0.66	3.13	74	0.7	0.64	8.57
19	0.2	0.22	10.0	47	0.72	0.67	6.94	75	0.66	0.63	4.55
20	0.13	0.13	0.00	48	0.59	0.64	8.47	76	0.52	0.46	11.54
21	0.51	0.49	3.92	49	0.61	0.67	9.84	77	0.5	0.43	14.00
22	0.52	0.51	1.92	50	0.63	0.64	1.59	78	0.48	0.46	4.17
23	0.1	0.15	16.67	51	0.2	0.22	0.00	79	0.4	0.46	4.55

	8				2				4		
24	0.46	0.46	0.00	52	0.2	0.21	5.00	80	0.65	0.71	9.23
25	0.73	0.66	9.59	53	0.23	0.21	8.70	81	0.47	0.49	4.26
26	0.44	0.43	2.27	54	0.48	0.45	6.25	82	0.49	0.46	6.12
27	0.21	0.21	0.00	55	0.49	0.51	4.08	83	0.6	0.63	5.00
28	0.4	0.46	15.00	56	0.24	0.23	4.17				

Average percentage of prediction error 6.48

Step four (4): The following step to optimize the neural network parameter is defining the number of hidden layer. Minimum one node and maximum three nodes of hidden layers were setup for this model. Based on [8] a few hidden layers may cause a high training error due to under-fitting and too many hidden layers may cause a high generalization error due to over-fitting. So, in this case the optimal numbers of hidden layer are determined by which layer that gives less average predicting error and the best configuration was observed with two hidden layers.

Step five (5): Then the next neural network parameter to be optimized is goal parameter. Goal or known as error goal related to both the convergence and accuracy of the ANN model [10]. For this optimization model, three goal parameters have been set which are goal 0 (default), goal 0.001 and goal 0.0001. The selected goal parameter is based on literature [10]. So the better goal parameter is 0.0001 which gives minimum average predicting error.

Step six (6): The last step optimization of neural network parameter is choosing neuron number. Neuron number has an influence in the accuracy of the ANN model [10]. Thus, neuron number count of 5, 10, 15 and 20 are used to investigate the reliability of the proposed ANN model. Thus, in this case, neuron number is chosen thru the above step where 15 number of neuron is selected as illustrated in (Figure 5).

5.2. ANN prediction

The neural network model has been developed via network type of feed-forward back-propagation with architecture 5-15-1 neurons. In this model, out of the 96 experimental data in Table 5, 83 data were considered for ANN training and the rest were used for ANN testing. The selection of data for training and testing was made by random method. Figure 6 shows the performance during development of model training. The ANN model training performance is based on the mean square error (MSE).

The training curve MSE shows a decreasing trend and this is a right training. While for the validation and test curves, it shows very similar trend. If the test curve had increased significantly before the validation curve increased, then it is possible that some over-fitting might have occurred [25]. The training was terminated when the validation error increased to 6 epochs, and the best validation performance was obtained as 0.00184 at epoch 3.

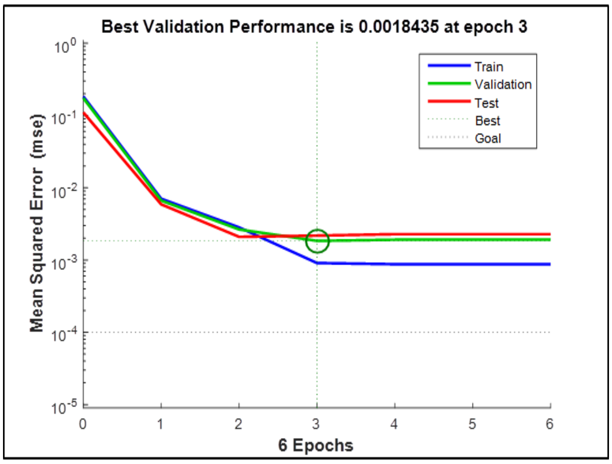

Fig. 6: Performance Plot of Groove Depth.

By referring Figure 7, it shows the coefficients of regression. The regression plots explain the relationship between the outputs of the network and the targets. The dashed line in each plot represents the targeted values while the solid line represents the best-fit linear regression between the outputs and targets.

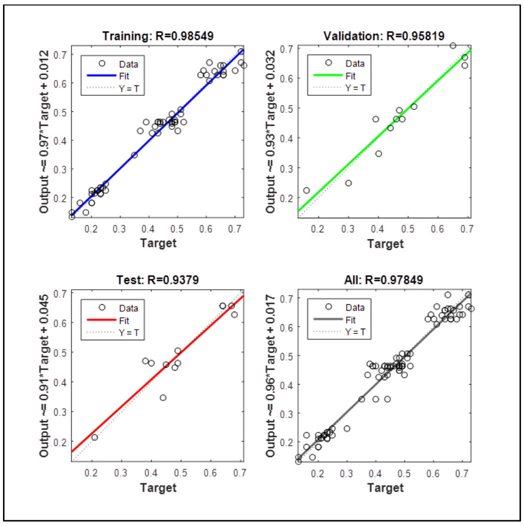

Fig. 7: Regression Plot of Groove Depth.

A good ANN model define as the value of correlation coefficient is maximum while the root mean square error is minimum [8]. Based on Figure 7 it was observed that the targeted output regression for training is 0.98549, validation is 0.95819, and testing is 0.9379. This means that the model has an exact linear relationship between outputs and targets because (R) is close to one.

The overall result shows that total response is 0.97849 and indirectly indicates that the ANN model output perfectly matches with the target. Table 6 shows the comparison between experimental and ANN training predicted for groove depth responses. Therefore as overall it shows that experimental and ANN predicted data training indicates good correlation where the average percentage prediction error value is 6.48% which is acceptable based on modelling standard [22]. However, a clear illustration between experimental and ANN predicted data training was shown in Figure 8.

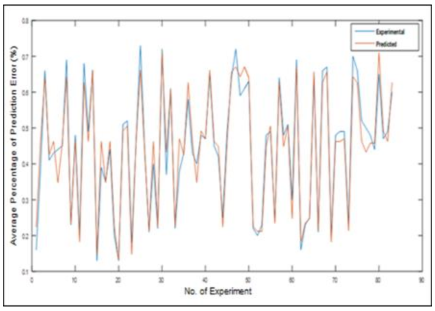

Fig. 8: The Comparative Signatures of the Groove Depth.

6. Conclusion

Investigation on modified CO2 laser cutting into 3D laser lathing has been done successfully. The machining characteristic, effect of parameter and significant effect against machining quality are the major issues in laser cutting domain. As to improve the parameter selection of laser cutting accuracy, an effective flow of ANN model selection has been developed in this research to model the experiment before come into actual environment. This is for better guidelines to produced desired quality machining on various critical part especially grooving side. In this study, modelling of laser cutting using ANN give better depth quality of micro-grooving. Results shows that, the optimised ANN model has predicted closely of the response, namely groove depth conducted by modified CO2 laser cutting machine. Throughout the modelling predictions, there was only one experimental run error is considered highest which is 37.50%, while the others are all below 20% of error where the calculated average error is found to be 6.48% which is much below than expected error about 10%, which often seen as acceptable range for modelling of machining processes. The reason being for one exceptional case would probably be due to experimental/human error in running the experimental. With this, it can be concluded that, ANN is very much suitable to model a nonlinear process such as laser cutting machine without any chance of deviating away from desired values.

Acknowledgement

The authors would like to thank Universiti Teknikal Malaysia Melaka, especially Faculty of Manufacturing Engineering (FKP), and Centre for Research and Innovation Management (CRIM) for providing us an enormous support technically and morally in getting this research completed as desired.

References

[1] Sivarao S, Peter Brevern, El-Tayeb N S M & Vengkatesh V C (2009), GUI based mamdani fuzzy inference system modeling to predict surface roughness in laser machining. *International Journal of Electrical & Computer Sciences IJECS-IJENS* 09 (09), pp. 37-43.

[2] Shoujin Sun & Milan Brandt (2013), Laser Beam Machining, Non-traditional Machining Processes, *SpringerVerlag* London.

[3] Romoli L, Tantussi G, & Dini G, (2007), Layered laser vaporization of PMMA manufacturing 3D mold cavities. *Annals of the CIRP* 56, pp. 209-212. https://doi.org/10.1016/j.cirp.2007.05.050.

[4] Young HT. Lin FF & Hong SB (2008), Novel approach to fabrication of 3D micro-structures by laser machining. *Key Engineering Materials* 364-366, I, pp. 19-24. https://doi.org/10.4028/www.scientific.net/KEM.364-366.19.

[5] Dhupal D, Doloi B, & Bhattacharyya B (2008), Pulsed Nd:YAG laser turning of micro-groove on aluminum oxide ceramic (Al2O3). *International Journal of Machine Tools & Manufacture* 48, pp. 236-248. https://doi.org/10.1016/j.ijmachtools.2007.08.016.

[6] Srijib Dhara Kr, Kuar A.S, Mitra S (2008), An artificial neural network approach on parametric optimization of laser micro-machining of die-steel. *International Journal Advanced Manufacturing Technology* 39, pp. 39-46. https://doi.org/10.1007/s00170-007-1199-1.

[7] Ranaganth BJ & Viswanath G, (2011), Application of artificial neural network for optimising cutting variables in laser cutting of 304 Grade stainless steel. *International Journal of Applied Engineering and Technology* 1 (1), pp.106-112.

[8] Waqas Saleem, Muhammad Zain-ul-abdein, Hassan Ijaz, Abdullah Salmeen Bin Mahfouz, Anas Ahmed, Muhammad Asad and Tarek Mabrouki (2017), Computational analysis and artificial neural network optimization of dry turning parameters—AA2024-T351. *Applied Sciences* 7, pp. 1-21. https://doi.org/10.3390/app7060642.

[9] Kbria1 G, Doloi B, & Bhattacharyya B (2014), Modelling and optimization of Nd:YAG laser micro-turning process during machining of aluminum oxide (Al2O3) ceramics using response surface methodology and artificial neural network. *Manufacturing Review* 1 (12), pp. 1-8. https://doi.org/10.1051/mfreview/2014011.

[10] Ming-Jong Tsai, Chen-Hao Li, & Cheng-Che Chen (2008), Optimal laser-cutting parameters for QFN packages by utilizing artificial neural networks and genetic algorithm. *Journal of Materials Processing Technology* 208, pp. 270-283. https://doi.org/10.1016/j.jmatprotec.2007.12.138.

[11] Miloš J. Madić & Miroslav R. Radovanović (2011), Optimal Selection of ANN Training and Architectural Parameters Using Taguchi Method: A Case Study. *FME Transactions* 39 (2), pp. 79-86.

[12] Nukman Y, Hassan MA & Harizam MZ (2013), Optimization of prediction error in co2 laser cutting process by taguchi artificial neural network hybrid with genetic algorithm. *Applied Mathematics & Information Sciences* 7 (1), pp. 363-370. https://doi.org/10.12785/amis/070145.

[13] Rama Bhadri Raju Chekuri, Ramakotaiah Kalluri, Rajesh Siriyala, & Jamaleswara kumar Palakollu (2018), A study on die sinking EDM of Nimonic C-263 super alloy: an intelligent approach to predict the process parameter using ANN. *International Journal of Engineering & Technology* 7 (1.1), pp. 651-654. https://doi.org/10.14419/ijet.v7i1.1.10796.

[14] Sathish S, Parthiban A, Balakrishna R, & Anandan R (2018), Development of ANN models for optimization of methane yield from floating dome digester. *International Journal of Engineering & Technology* 7 (2.21) 316-318. https://doi.org/10.14419/ijet.v7i2.21.12393.

[15] Nurul Sulaiha Sulaiman, Khairiyah Mohd-Yusof, & Asngari Mohd-Saion (2018), Quality prediction modeling of palm oil refining plant in Malaysia using artificial neural network models. *International Journal of Engineering & Technology* 7 (3.26), 19-22.

[16] Chryssolouris G, *Laser Machining* Mechanical Engineering Series. New York: Springer, 1991, pp. 160-208. https://doi.org/10.1007/978-1-4757-4084-4_5.

[17] Schulz W, Simon G, Urbassek HM, & Decker I (1987), On laser fusion cutting of metals. *J. Phys. D: Applied Physics* 20, pp. 481-488. https://doi.org/10.1088/0022-3727/20/4/013.

[18] Bunting KA, & Cornfield G (1975), Toward a general theory of cutting: a relationship between the incident power density and the cut speed. *Journal of Heat Transfer*, pp. 116-122. https://doi.org/10.1115/1.3450258.

[19] Petring, D, Abels P, Beyer E, & Herziger G (1988), Werkstoffbearbeitung mit Laserstrahlung. *Feinwerktechnik & Messtechnik* 96, pp. 364-372.

[20] Chinmay KD, & Abdulhafiz S (2012), Prediction of depth of cut for single-pass laser micro-milling process using semi-analytical, ANN and GP approaches. *International Journal Advanced Manufacturing Technology* 60, pp. 865–882. https://doi.org/10.1007/s00170-011-3677-8.

[21] Bappa A, Subrata M, Bipan T, & Dipten M (2011), Application of artificial neural network for predicting weld quality in laser transmission welding of thermoplastics. *Applied Soft Computing* 11, pp. 2548–2555. https://doi.org/10.1016/j.asoc.2010.10.005.

[22] Sivarao, Peter Brevern, N.S.M. El-Tayeb & Vengkatesh VC (2009), Modeling, testing and experimental validation of laser machining micro quality response by artificial neural network. International Journal of Engineering & Technology IJET-IJENS 09 (09), pp. 24-29.

[23] Yusliza Yusoff, Azlan Mohd Zain, Safian Sharif, Roselina Sallehuddin, (2016), Potential ANN prediction model for multiperformances WEDM on Inconel 718. Neural computing & application 30 (7), pp. 2113-2127. https://doi.org/10.1007/s00521-016-2796-4.

[24] Miloš Madic & Miroslav Radovanovic (2012), An artificial intelligence approach for the prediction of surface roughness in co2 laser cutting. Journal of Engineering Science and Technology 7 (6), pp. 679 – 689. https://doi.org/10.5897/IJPS12.109.

[25] Mark HB, Martin TH & Howard BD. "Neural Network Toolbox User's Guide", available online https://www. mathworks.com/ help/pdf_doc/nnet /nnet_ug.pdf, last visit 20.02 2018.